**ALCHEMY Jurnal Penelitian Kimia**

Official Website: https://jurnal.uns.ac.id/alchemy

ISSN 1412-4092
EISSN 2443-4183

# Agricultural Residues as Alternative Feedstocks for Nanocrystalline Cellulose (NCC): Comparative Analysis of Empty Fruit Bunch Oil Palm, Bagasse, and Pineapple Crowns

**Muhammad Muhammad[a*], Eka Marya Mistar[a], Khairul Rahmah[b], Edi Munawar[b], Fitriani Fitriani[c]**

[a]*Department of Chemical Engineering, Faculty of Engineering, Universitas Serambi Mekkah*
*Jalan Tgk. Imum Lueng Bata, Batoh, Banda Aceh 23245, Indonesia*
[b]*Department of Chemical Engineering, Faculty of Engineering, Universitas Syiah Kuala*
*Jalan Syech Abdurrauf No.7, Darussalam, Banda Aceh 23111, Indonesia*
[c]*Research Center for Biomass and Bioproduct, National Research and Innovation Agency (BRIN)*
*Jalan Raya Puspiptek No. 60, Setu, South Tangerang 15314, Indonesia*

[*]*Corresponding author: muhammad@serambimekkah.ac.id*

*DOI: 10.20961/alchemy.22.2.109364.349-361*

*Received 27 September 2025, Revised 15 June 2026, Accepted 28 June 2026, Published 30 September 2026*

**Keywords:**

cellulose;
crystal size;
crystallinity;
functional group;
morphology;
yield.

**ABSTRACT.** Nanocrystalline cellulose (NCC) was successfully isolated from three tropical agricultural residues oil palm empty fruit bunch (EFB), sugarcane bagasse (SB), and pineapple crown leaves (PCL) via acid hydrolysis. The influence of feedstock lignocellulosic composition on NCC yield, crystallinity, thermal stability, surface chemistry, and morphology was systematically evaluated using gravimetric analysis, Fourier-transform infrared spectroscopy (FTIR), X-ray diffraction (XRD), thermogravimetric analysis (TGA), and scanning electron microscopy (SEM). PCL, which exhibited the highest cellulose content (60.49%) and the lowest lignin fraction (15.24%) among the three feedstocks, yielded the highest NCC recovery (70.37 ± 1.10%), the greatest crystallinity index (CrI = 73.57%), the highest thermal decomposition onset temperature (291 °C), and a rod-like morphology closely approaching that of commercial NCC. In contrast, SB and EFB produced substantially lower NCC yields (33.23 ± 1.86% and 36.17 ± 0.91%, respectively), reduced crystallinity (70.25% and 68.31%), lower thermal stability onset temperatures (285 °C and 280 °C), and more heterogeneous particle morphologies, attributable to their elevated lignin and hemicellulose burdens that impede reagent penetration during pretreatment and hydrolysis. FTIR analysis confirmed the effective removal of non-cellulosic components across all samples. These findings establish a feedstock compositional hierarchy (PCL > SB > EFB) governing NCC.

## INTRODUCTION

Cellulose is recognized as a natural polymer that is abundant on Earth and a renewable, advanced material (Shen *et al.*, 2022). Cellulose is a linear polysaccharide characterized by a structural arrangement of β-D-glucopyranose units connected via β (1-4) glycosidic bonds (Liu *et al.*, 2022). The cellulose structure consists of alternating crystalline and amorphous regions, which fundamentally govern its physicochemical properties and determine its potential for material applications. This structure is greatly influenced by the method used to extract it. One of the most used processes is acid hydrolysis (Magalhães *et al.*, 2023).

Acid hydrolysis is an advanced approach to isolating cellulose components because it selectively breaks down the amorphous part of cellulose without damaging the crystalline structure, resulting in nanocellulose with a homogeneous particle-size distribution and rod-shaped nanoparticles called nanocrystalline cellulose (NCC) (Almashhadani *et al.*, 2022). The resulting NCC is a nano-scale particle with remarkable properties, including a high crystallinity index, a large surface area, and a superior biocompatibility profile. These unique properties of NCC have positioned it as a versatile nanomaterial with broad application potential in various industries (Madhushree *et al.*, 2024).

**Cite this as:** Muhammad, M., Mistar, E. M., Rahmah, K., Munawar, E., and Fitriani, F. (2026). Agricultural Residues as Alternative Feedstocks for Nanocrystalline Cellulose (NCC): Comparative Analysis of Empty Fruit Bunch Oil Palm, Bagasse, and Pineapple Crowns. *ALCHEMY Jurnal Penelitian Kimia*, 22(2), 349-361. doi: https://dx.doi.org/10.20961/alchemy.22.2.109364.349-361.



Copyright © 2026, Universitas Sebelas Maret, ISSN 1412-4092, e ISSN 2443-4183

Comprehensive studies on various biomass sources have been prompted by the scientific field's rising interest in NCC. Among them, researchers have successfully extracted NCC from conventional raw materials, including wood pulp, rice straw, banana fiber, coconut fiber, palm trunks, corn straw residues, and pea pod waste (Ansari *et al.*, 2024). This diversification of raw materials reflects the growing demand for sustainable nanomaterials and the need to identify economic and region-specific raw materials.

Although research on nanocrystalline cellulose (NCC) continues to evolve, a considerable knowledge gap exists regarding the systematic evaluation of tropical agricultural waste as a potential raw material. This limitation is particularly evident in regions with intensive agricultural activity that generate large biomass residues. Indonesia, for example, is one of the world's largest agricultural countries, and the agricultural sector is a major pillar of the economy, producing millions of tons of biomass waste each year (Qureshi *et al.*, 2024).

Abundant by-products, such as empty palm fruit bunches (EFB), bagasse, and pineapple crowns, remain largely underutilized. Common management practices include open burning, uncontrolled disposal on land, or simple processing into low-value compost and animal feed. This approach not only causes the loss of potential utilization of cellulose-rich resources but also exacerbates environmental problems. Thus, the utilization of tropical agricultural waste to produce value-added materials, such as NCC, offers strategic opportunities in supporting sustainability while reducing the negative impacts of inefficient waste management (Nahurira *et al.*, 2024).

A critical consideration in NCC research involves understanding how the composition of raw materials affects the properties of the resulting nanomaterials. Palm oil EFB, bagasse, and pineapple crowns, while all containing significant cellulose fractions, have different composition profiles in terms of hemicellulose and lignin content. Furthermore, these materials exhibit varying fiber morphologies and structural organization at the microscopic level. These differences in composition and structure are expected to significantly influence key NCC characteristics, including extraction yield, crystallinity index, dimensional properties, and surface functionality. However, comprehensive comparative studies analyzing these three specific residues are still very rare in the literature, creating uncertainty about their relative advantages as NCC feedstocks (Alvarado *et al.*, 2024).

To address this important knowledge gap, this study systematically compared NCC extraction from palm oil fruit waste (EFB), sugarcane waste, and pineapple crown waste through a controlled acid hydrolysis protocol. This study employs a comprehensive characterization approach, using extraction yield analysis, Fourier transform infrared spectroscopy (FTIR), X-ray diffraction (XRD), and scanning electron microscopy (SEM) to reveal structure-property relations.

## RESEARCH METHODS

Oil palm empty fruit bunch (EFB) fibers, sugarcane bagasse, and pineapple crown leaves were collected from local agricultural waste in Aceh, Indonesia. Sodium hydroxide (NaOH, 98%, Merck, Germany), used for alkalization, was purchased from Sigma-Aldrich. Sodium hypochlorite (NaOCl, 12% active chlorine) for bleaching was obtained from Rudang Jaya, Medan, Indonesia. Sulfuric acid ($H_2SO_4$, 98%, Merck, Germany) was used for acid hydrolysis to obtain nanocrystalline cellulose. All reagents were of analytical grade and used without further purification.

### Experimental Setup

The raw biomass samples (EFB fibers, sugarcane bagasse (SB), and pineapple crown leaves (PCL)) were first washed thoroughly with distilled water, oven-dried at 60 °C, and ground to a particle size <1 mm. The powders were subjected to an alkalization treatment with 1 M NaOH solution at 80 °C for 2 h (solid-to-liquid ratio 1:20, w/v) to remove hemicellulose and extractives. After washing with distilled water until neutral pH, the fibers were bleached with 5 wt% NaOCl solution at 70 °C for 1 h. The bleaching step was repeated twice to reduce lignin content, yielding purified cellulose with a whitish appearance. The obtained cellulose was then hydrolyzed using 3 M $H_2SO_4$ at 45 °C for 3 h under vigorous stirring (solid-to-liquid ratio 1:10, w/v). The hydrolysis was quenched by adding tenfold cold distilled water, followed by centrifugation at 10,000 rpm for 15 min. The washing centrifugation cycle was repeated until the supernatant reached near-neutral pH. Finally, the NCC was dried to obtain nanoparticle powders (Figure 1).



Copyright © 2026, Universitas Sebelas Maret, ISSN 1412-4092, e ISSN 2443-4183

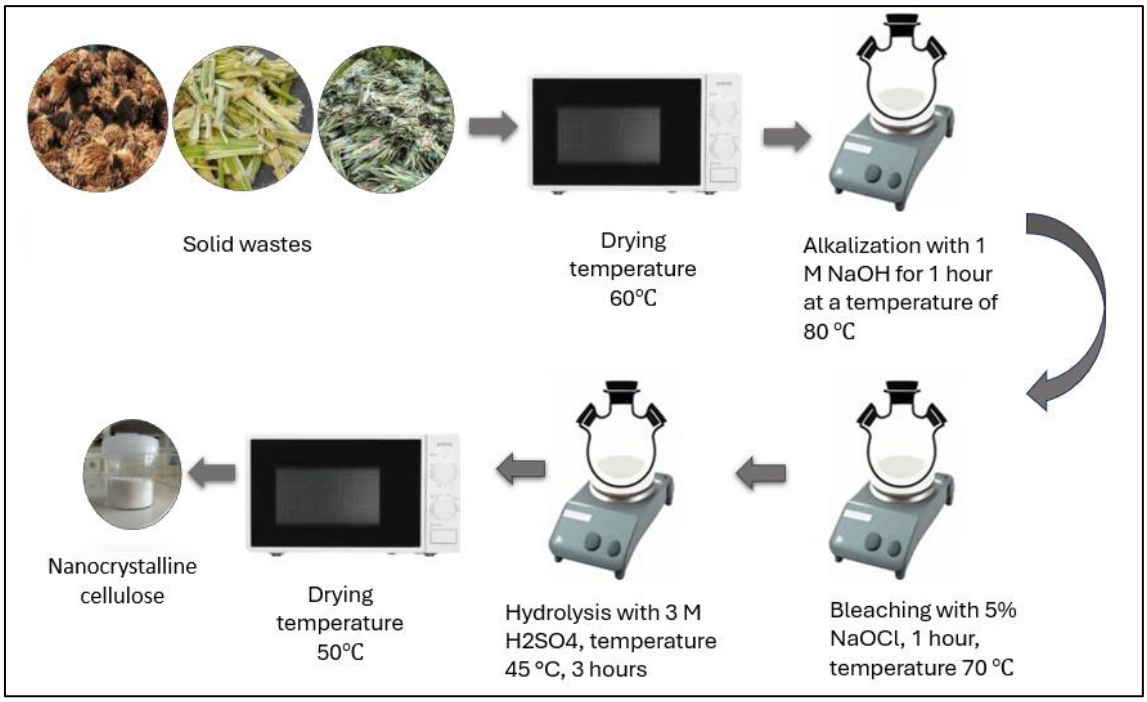



**Figure 1.** Illustration of the process of isolation nanocrystalline cellulose.

**Chemical Characterization**

The chemical composition of pineapple crown leaf fiber (PCL), sugarcane bagasse (SB), and empty fruit bunch (EFB) was determined using the Chesson-Datta method in accordance with the procedure reported by (Alsuwait *et al.*, 2024).

***Cellulose Content***

The cellulose content of untreated and chemically treated PCL, SB, and EFB fibers was determined following the Kushner-Hoffer procedure. In this method, a pre-weighed fiber sample ($W_1$) was immersed in a mixture of ethanol and nitric acid at a 4:1 (v/v) ratio for 4 h to dissolve non-cellulosic components. The remaining residue was then oven-dried at 60 °C until a constant weight ($W_2$) was achieved. The cellulose content was calculated as a weight percentage using Equation 1.

$$\% \text{ Cellulose} = \left(\frac{W_2}{W_1}\right) \times 100 \quad (1)$$

***Hemicellulose Content***

The hemicellulose content of untreated and chemically treated PCL, SB, and EFB fibers was determined by alkaline extraction. Pre-weighed fiber samples ($W_1$) were soaked in a 5 wt.% NaOH solution for 30 min at room temperature to dissolve the hemicellulose fraction, followed by neutralization with a dilute HCl solution. The residue was oven-dried at 105 °C for 2 h until a constant weight ($W_2$) was obtained. The hemicellulose content was calculated based on the mass difference before and after treatment, as given in Equation 2.

$$\% \text{ Hemicellulose} = (W_1 - W_2) \times 100 \quad (2)$$

***Lignin Content***

The lignin content of untreated and chemically treated PCL, SB, and EFB fibers was evaluated according to ASTM D 1106-96. Prior to analysis, extractives were removed from the fiber samples using a Soxhlet apparatus with an ethanol–toluene solvent mixture (1:2, v/v) for 8 h. Subsequently, 1 g of the pre-extracted sample was hydrolyzed in 72% $H_2SO_4$ for 2 h, diluted with distilled water, and then refluxed for an additional 4 h. The acid-insoluble residue was filtered, washed with distilled water until a neutral pH was reached, and oven-dried at 103 °C for 2 h. The lignin content was calculated using Equation 3.

$$\% \text{ Lignin} = \left(\frac{W_{residue}}{W_{sample}}\right) \times (100 - W_3 \quad (3)$$

where $W_3$ represents the ash content (%) of the sample determined by thermogravimetric analysis at 575 °C.



Copyright © 2026, Universitas Sebelas Maret, ISSN 1412-4092, e ISSN 2443-4183

**Percentage Yield**

The percentage yield of nanocrystalline cellulose was determined to evaluate the efficiency of the hydrolysis process. The calculation was performed using the following Equation 4.

$$\text{Yield } (\%) = \frac{W_2}{W_1} \times 100\% \quad (4)$$

where $W_1$ represents the initial dry weight of cellulose before acid hydrolysis, and $W_2$ denotes the dry weight of the obtained nanocrystalline cellulose after the completion of the hydrolysis, washing, and drying steps. This approach provides a straightforward estimation of the conversion efficiency from raw cellulose to nanocrystals. A higher yield indicates that a larger fraction of the starting cellulose material was successfully converted into nanoscale crystals, whereas a lower yield may suggest incomplete hydrolysis or potential material loss during purification and recovery. Such yield calculations are essential for comparing different preparation methods and optimizing process parameters to achieve maximum efficiency (Mishra *et al.*, 2023).

**Functional Group and Chemical Structure Analysis**

FTIR spectroscopy was employed to analyze the chemical structure of the samples. The spectra were recorded within the range of 4000 – 400 $cm^{-1}$ at a resolution of 4 $cm^{-1}$, allowing the identification of functional groups, verification of lignin and hemicellulose removal after pretreatment, and detection of possible chemical changes induced by hydrolysis (Fitriani *et al.*, 2022).

**Crystalline Structure and Crystallinity Characterization**

The crystalline phase of cellulose and NCC samples was analyzed by X-ray diffraction (XRD) using Cu Kα radiation (λ = 1.5406 Å) at 40 kV and 30 mA. Diffraction patterns were collected over the 2θ range of 5 – 40°. The crystallinity index (CrI) was determined following the Segal method to evaluate structural ordering before and after hydrolysis (Akinjokun *et al.*, 2021). The degree of crystallinity was calculated using Equation 5, while the crystallite size was obtained from Equation 6.

$$\text{CrI} = \frac{I_{200} - I_{am}}{I_{200}} \times 100 \quad (5)$$

Where CrI is the crystallinity index, $I_{200}$ indicates the diffraction intensity at the highest crystalline peak, and $I_{am}$ indicates the diffraction intensity of the amorphous region.

$$D\ (2\theta) = \frac{K\lambda}{\beta cos\theta} \quad (6)$$

Where $D$ is the average particle size, $\beta$ is the Full width at half maximum (FWHM) (rad), $\theta$ is the Bragg angle (°), $K$ is the dimensionless factor (0.9), and $\lambda$ is the X-ray wavelength (0.1541 nm) Cu-Kα.

**Thermogravimetric Analysis (TGA)**

The thermal stability and degradation behavior of the fiber samples were investigated by thermogravimetric analysis (TGA) using a TA Instruments Q500 thermal analyzer (TA Instruments, USA). Approximately 5 – 10 mg of each oven-dried powdered sample was placed in a tared platinum crucible and subjected to controlled heating from ambient temperature to 600 °C at a constant heating rate of 10 °C/min under an inert nitrogen atmosphere maintained at a purge flow rate of 50 mL/min. Continuous nitrogen purging was employed to prevent oxidative degradation during the analysis, thereby ensuring that the observed mass loss events were solely attributable to thermal decomposition mechanisms. The mass loss (TGA) curves were continuously recorded and subsequently analyzed to identify and delineate the characteristic decomposition stages associated with the constituent biopolymeric components of the fibers, namely hemicellulose, cellulose, and lignin (D'Acierno *et al.*, 2023).

**Surface Morphology and Microstructure Evaluation**

The surface morphology of NCC samples obtained after acid hydrolysis was examined using scanning electron microscopy (SEM). Dried powders were mounted on aluminum stubs with conductive carbon tape and sputter-coated with a thin layer of gold to improve conductivity. SEM imaging was carried out at an accelerating voltage of 15 kV. The micrographs revealed nanoscale structural features, indicating fragmentation of cellulose microfibers into smaller crystalline domains. The observed reduction in particle size and formation of more homogeneous structures confirmed the effectiveness of the hydrolysis treatment in producing NCC (Sartika *et al.*, 2023).



(cc) BY-NC Copyright © 2026, Universitas Sebelas Maret, ISSN 1412-4092, e ISSN 2443-4183

## RESULTS AND DISCUSSION

### Lignocellulosic Composition of Raw Feedstocks

The chemical composition of a lignocellulosic feedstock is the primary determinant of NCC extraction efficiency, as it governs the degree of delignification achievable during pretreatment and the fraction of crystalline cellulose available for hydrolytic conversion. The measured compositions of the three agricultural residues are summarized in Table 1.

**Table 1.** Lignocellulosic composition of raw feedstocks (PCL = pineapple crown leaves; SB = sugarcane bagasse; EFB = empty fruit bunch).

| Sample | Hemicellulose (%) | Cellulose (%) | Lignin (%) | Ash (%) |
|---|---|---|---|---|
| PCL | 21.35 | 60.49 | 15.24 | 2.92 |
| SB | 15.42 | 41.82 | 39.52 | 3.24 |
| EFB | 28.08 | 33.27 | 32.14 | 2.51 |

Pineapple crown leaves exhibited the highest cellulose content (60.49%) among the three feedstocks, accompanied by a relatively modest lignin loading of 15.24% and a hemicellulose fraction of 21.35%. This compositional profile is particularly advantageous for NCC production: the elevated cellulose fraction maximizes the theoretical NCC yield, while the low lignin content reduces the chemical severity required during bleaching, minimizing the risk of unintended oxidative degradation of the cellulose chains (Faria *et al.*, 2020). The ash content of PCL (2.92%) was within the typical range for herbaceous fibers and is not expected to impede processing.

Sugarcane bagasse exhibited a substantially lower cellulose fraction (41.82%) and an elevated lignin content of 39.52%, the highest among the three materials investigated. This high lignin burden is mechanistically significant: lignin forms covalent and non-covalent cross-links with cellulose microfibrils that resist dissolution under mild alkaline conditions, necessitating more intensive and repeated delignification treatments to expose the underlying cellulose. The comparatively low hemicellulose fraction of SB (15.42%) may be attributed to partial hemicellulose hydrolysis during the bagasse-processing stage at the sugarcane mill (Mahmud and Anannya, 2021).

Empty fruit bunches of oil palm displayed the highest hemicellulose content (28.08%) alongside the lowest cellulose fraction (33.27%) of the three feedstocks. The co-occurrence of high hemicellulose and significant lignin (32.14%) in EFB reflects the mature, densely cross-linked vascular fiber bundles characteristic of monocotyledonous palm tissue. Hemicellulose is predominantly amorphous and randomly oriented; its prevalence both dilutes the cellulosic fraction and, when incompletely removed, tends to disrupt the crystalline packing of cellulose in the extracted NCC (Dimawarnita *et al.*, 2023). Taken together, the compositional data establish a clear hierarchy, PCL > SB > EFB, in terms of suitability as a primary cellulosic feedstock for high-yield NCC production.

### Percentage Yield

The gravimetric yield of nanocrystalline cellulose (NCC) recovered following sulfuric acid hydrolysis differed markedly among the three agricultural residue feedstocks, as summarized in Table 2. Pineapple crown leaves (PCL) delivered the highest NCC yield of 70.37 ± 1.10% (superscript a), a value that is statistically distinguishable from both sugarcane bagasse (SB: 33.23 ± 1.86%) and oil palm empty fruit bunch (EFB: 36.17 ± 0.91%), which were not significantly different from each other (superscript b; $p < 0.05$, one-way ANOVA with Tukey HSD post hoc test). The nearly twofold superiority of PCL over SB and EFB is a direct quantitative expression of the compositional hierarchy established in Section 3.1: PCL carries the highest cellulose content (60.49%) and the lowest lignin fraction (15.24%) among the three feedstocks, parameters that collectively govern the efficiency of the acid hydrolysis step. Because NCC yield is calculated relative to the dry cellulose input, feedstocks with a greater proportion of accessible, high-purity cellulose will inherently return a larger mass of crystalline nanoparticles per unit of biomass processed (Fitriani *et al.*, 2021). In contrast, the substantially lower NCC recoveries from SB (33.23 ± 1.86%) and EFB (36.17 ± 0.91%) are mechanistically attributable to their elevated lignin and hemicellulose burdens SB: lignin 39.52%, hemicellulose 15.42%; EFB: lignin 32.14%, hemicellulose 28.08% which impede acid penetration into the fiber matrix, encapsulate cellulose microfibrils within a resistant lignin–hemicellulose sheath, and thereby protect a significant fraction of the cellulosic material from hydrolytic attack (Mahmud and Anannya, 2021; Dimawarnita *et al.*, 2023). The absence of a statistically significant difference between SB and EFB yields (both sharing superscript b in Table 2) further suggests that,



Copyright © 2026, Universitas Sebelas Maret, ISSN 1412-4092, e ISSN 2443-4183

beyond a threshold lignin content of approximately 32%, incremental increases in lignin loading do not proportionally suppress NCC yield under the mild hydrolysis conditions employed here, an observation consistent with reports indicating that the physical accessibility of cellulose microfibrils governed by fiber morphology and delignification efficiency exerts a greater influence on yield than absolute lignin content alone (Hidayatulloh *et al.*, 2025).

**Table 2.** Percentage yield of NCC.

| Sample | Yield (%) |
|---|---|
| NCC pineapple crown leaves (PCL) | $70.37 \pm 1.10^{a}$ |
| NCC sugarcane bagasse (SB) | $33.23 \pm 1.86^{b}$ |
| NCC oil palm empty fruit bunch (EFB) | $36.17 \pm 0.91^{b}$ |

Taken together, these data confirm that the pretreatment sequence employed in the present study, sequential alkalization and bleaching followed by acid hydrolysis, is effective for PCL but insufficiently aggressive to fully overcome the recalcitrant lignocellulosic architecture of SB and EFB under the mild conditions applied, consistent with the view that delignification efficiency, rather than acid hydrolysis duration alone, is the primary process lever governing NCC yield from high-lignin feedstocks (Hidayatulloh *et al.*, 2025).

The observed yield hierarchy (PCL > EFB > SB) is also noteworthy from a process economics perspective. The narrow standard deviations of all three measurements (±1.10%, ±1.86%, and ±0.91% for PCL, SB, and EFB, respectively) confirm the reproducibility of the acid hydrolysis protocol across independent replicates, lending confidence to the comparative conclusions. The relatively larger variability in SB yield (±1.86%) likely reflects the heterogeneous distribution of residual lignin in bagasse particles that escaped complete delignification, resulting in batch-to-batch fluctuations in the proportion of cellulose accessible to the acid. Contextualizing these yields against the broader literature, the PCL value of 70.37% is among the higher recoveries reported for agricultural residue-derived NCC produced by $H_2SO_4$ hydrolysis under ambient-pressure conditions, comparable to the 79.37% yield reported by Fitriani *et al.* (2020) for pineapple crown fibers hydrolyzed for one hour, and substantially exceeding the 30 – 37% yields documented for EFB-derived NCC under one-pot catalytic conditions (Hidayatulloh *et al.*, 2025). The EFB yield of 36.17% obtained in the present study aligns closely with this reference range, further validating the experimental methodology. Collectively, these findings establish that pineapple crown leaves, by virtue of their inherently favorable lignocellulosic composition, represent the most efficient and reproducible among the three tropical agricultural residues investigated for sustainable, high-yield NCC production under mild acid hydrolysis conditions (Akhlaq *et al.*, 2022; Sayakulu and Soloi, 2022).

**Functional Groups**

The FTIR spectra of NCC obtained from pineapple crown, bagasse, EFB, and commercial reference exhibit similar characteristic absorption bands, indicating that the cellulose backbone was preserved after extraction in Figure 2. The broad band around 3300 $cm^{-1}$ corresponds to O-H stretching vibrations, confirming the hydroxyl groups responsible for hydrogen bonding and hydrophilic character. A slight shift to lower wavenumbers in NCC from pineapple crown suggests stronger hydrogen bonding and increased crystallinity after hydrolysis, consistent with previous studies on NCC from rice husk and kenaf bast (Pérez *et al.*, 2022; Dungani *et al.*, 2023). The peaks at 2850 – 2950 $cm^{-1}$ are assigned to C–H stretching of $CH_2$ groups in the glucose units, with no significant variation among samples.

The weak band near 1640 $cm^{-1}$ is attributed to O–H bending of absorbed water, while the absence of peaks at 1500 – 1600 $cm^{-1}$ and 1730 $cm^{-1}$ confirms the effective removal of lignin and hemicellulose during pretreatment (Hidayatulloh *et al.*, 2021). Strong absorptions in the region 1000 – 1150 $cm^{-1}$ are associated with C–O–C stretching of glycosidic bonds, reflecting the intact cellulose molecular structure (Fitriani *et al.*, 2020). Overall, the spectra of NCC derived from agricultural residues closely resembles that of commercial NCC, confirming successful removal of non-cellulosic components and retention of the cellulose crystalline framework.



Copyright © 2026, Universitas Sebelas Maret, ISSN 1412-4092, e ISSN 2443-4183

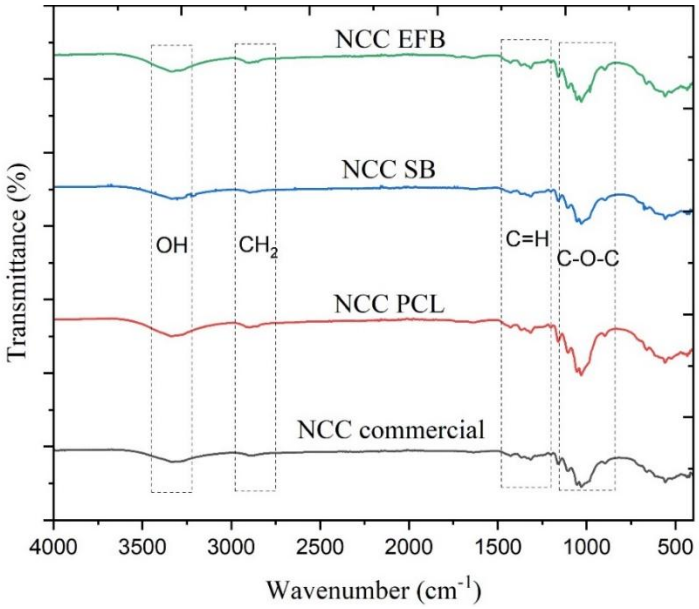



**Figure 2.** FTIR nanocrystalline cellulose (NCC).

**Crystallinity**

All samples exhibited the characteristic diffraction peaks of cellulose I at $2\theta \approx 16°$, 22 – 23°, and 35° (Figure 3), confirming that the crystalline allomorph was preserved after pretreatment and hydrolysis. The corresponding crystallinity index (CrI) values and crystallite sizes are presented in Table 3. Among the samples, commercial NCC showed the highest CrI (79.18%), followed by pineapple crown (73.57%), sugarcane bagasse (70.25%), and EFB (68.31%). This sequence reflects the naturally higher cellulose fraction in pineapple crown leaves and the more efficient removal of amorphous domains compared to bagasse and EFB. Comparable correlations between feedstock composition and crystallinity have also been reported in recent studies (Hemida *et al.*, 2023).

Crystallite size showed the opposite trend, being smaller for commercial (1.05 nm) and pineapple crown NCC (1.82 nm), but larger for bagasse (1.99 nm) and EFB (2.06 nm). This suggests that pineapple crown leaves allow a more efficient cleavage of amorphous regions, generating denser and finer crystallites, whereas the complex lignocellulosic structure of bagasse and EFB hindered uniform hydrolysis, leading to aggregation and larger apparent crystallites (Dimawarnita *et al.*, 2023). Similar observations were reported by Mtibe *et al.* (2022), who found that agricultural residues with higher lignin and hemicellulose content typically yield lower CrI values and coarser crystallite dimensions due to incomplete disruption of amorphous matrices. In contrast, residues with relatively simple fiber arrangements, such as pineapple crown leaves, are more prone to effective acid hydrolysis, leading to higher crystallinity (Fitriani *et al.*, 2022).

From an application perspective, higher crystallinity is associated with greater stiffness and thermal stability, while smaller crystallites increase surface reactivity. Pineapple crown NCC, therefore, provides a favorable balance, aligning with previous reports highlighting its potential as a reinforcement in polymer nanocomposites (Rodzi *et al.*, 2024).

**Table 3**. Crystallinity percentage and crystal size of NCC.

| Samples | Crystallinity (%) | Crystal size (nm) |
|---|---|---|
| NCC commercial | 79.18 | 1.05 |
| NCC pineapple crown leaves (PCL) | 73.57 | 1.82 |
| NCC sugarcane bagasse (SB) | 70.25 | 1.99 |
| NCC oil palm empty fruit bunch (EFB) | 68.31 | 2.06 |



Copyright © 2026, Universitas Sebelas Maret, ISSN 1412-4092, e ISSN 2443-4183

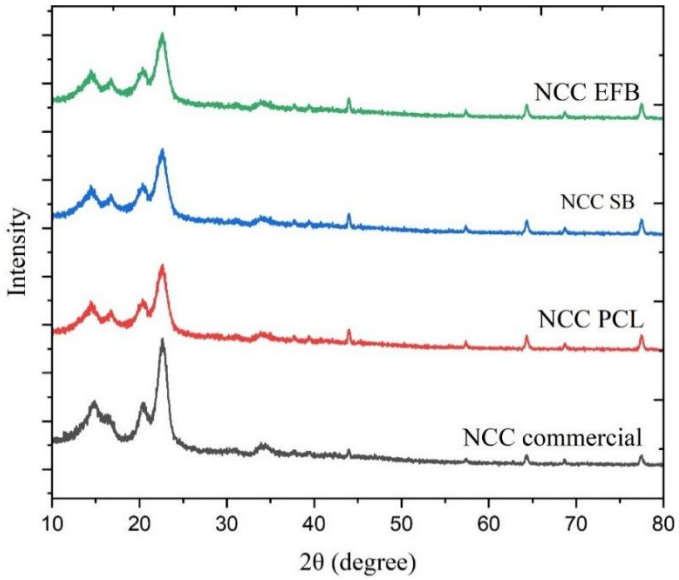



**Figure 3.** XRD of nanocrystalline cellulose (NCC).

**Thermogravimetric Analysis (TGA)**

The thermal degradation behavior of the four NCC types, as revealed by TGA under nitrogen atmosphere, followed a characteristic three-stage pattern (Figure 4), and the key thermal parameters are summarized in Table 4. In the first stage (30 – 120 °C), all samples exhibited a minor mass loss of approximately 5%, attributable to the evaporation of physically and weakly bound surface moisture. The comparable magnitude of this dehydration event across all samples indicates similar initial moisture contents, consistent with the hygroscopic character of nanocellulosic materials bearing abundant surface hydroxyl groups (Khan *et al.*, 2021).

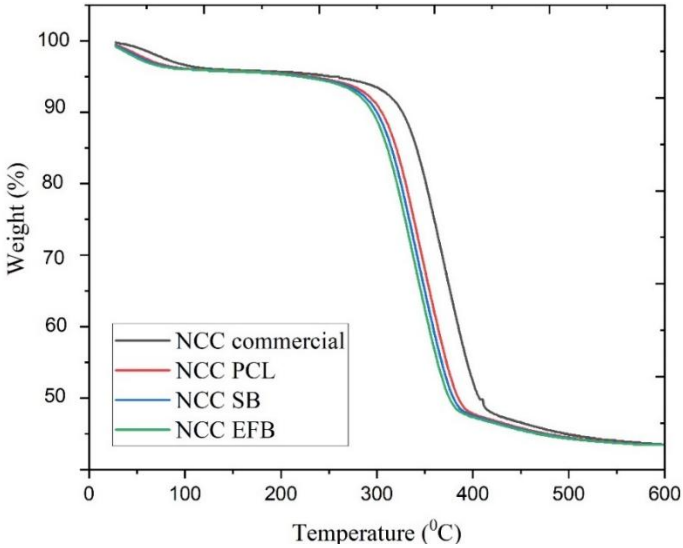



**Figure 4**. TGA of nanocrystalline cellulose (NCC).

The dominant degradation event in the second stage (280 – 400 °C) is assigned to the primary thermal decomposition of crystalline cellulose, involving glycosidic bond cleavage, dehydration of glucopyranose units, depolymerization of cellulose chains, and progressive oxidative char formation (D'Acierno *et al.*, 2023). The onset temperature of this degradation stage is a key indicator of thermal stability, decreasing in the order: commercial NCC (293 °C) > PCL-NCC (291 °C) > SB-NCC (285 °C) > EFB-NCC (280 °C). This ranking closely parallels the crystallinity hierarchy established by XRD: the more highly ordered crystalline lattice of PCL-NCC requires a greater thermal input to initiate chain scission and depolymerization than the less crystalline, more disordered structures of SB-NCC and EFB-NCC. It is also noteworthy that surface sulfate groups introduced by $H_2SO_4$ hydrolysis are known to catalyze dehydration reactions and reduce onset temperatures relative to unsulfated



Copyright © 2026, Universitas Sebelas Maret, ISSN 1412-4092, e ISSN 2443-4183

celluloses; the broadly similar onset temperatures across the four samples indicate comparable degrees of surface sulfonation under the standardized hydrolysis conditions employed (Solhi *et al.*, 2023).

Similarly, the temperature of maximum decomposition rate ($T_{max}$) followed the same trend: 399 °C (commercial) > 394 °C (PCL) > 390 °C (SB) > 382 °C (EFB). The lower $T_{max}$ values of SB- and EFB-derived NCC are consistent with their reduced crystallinity and the presence of residual amorphous material, which decomposes preferentially at lower temperatures than crystalline domains. In the third stage (>400 °C), all curves converged to stable residue levels of 32.1 – 33.2%, representing carbonaceous char and mineral ash, the latter originating from the inorganic constituents of the agricultural feedstocks (Harahap *et al.*, 2023). The near-identical residue fractions suggest that differences in char yield are not significantly influenced by feedstock origin under these conditions. Collectively, the TGA data confirm that PCL-derived NCC not only achieves the highest yield and crystallinity among the agricultural residue-derived materials but also exhibits thermal stability closely approaching that of commercial NCC, further validating its suitability as a drop-in replacement in high-temperature processing or thermally demanding application environments.

**Table 4.** Thermogravimetric parameters of NCC derived from agricultural residues and commercial reference.

| Sample | Onset (°C) | $T_{max}$ (°C) | Residue (%) |
|---|---|---|---|
| NCC commercial | 293 | 399 | 33.1 |
| NCC PCL | 291 | 394 | 33.2 |
| NCC SB | 285 | 390 | 32.8 |
| NCC EFB | 280 | 382 | 32.1 |

**Morphology Scanning Electron Microscopy (SEM)**

The surface morphology of NCC derived from commercial sources, pineapple crown leaves (PCL), sugarcane bagasse (SB), and oil palm empty fruit bunch (EFB) was examined by scanning electron microscopy (SEM), and the resulting micrographs are presented in Figure 5. All four panels were acquired at identical magnification (×80, scale bar = 200 μm), enabling direct cross-sample comparison of particle assemblies and aggregation behavior at the microscale. Pronounced morphological differences among the four samples are clearly discernible and are fully consistent with the compositional and structural trends established by FTIR, XRD, and TGA analyses.

Commercial NCC (Figure 5a) presents a bimodal morphological landscape comprising two coexisting populations: discrete, well-defined rod-like particles whose elongated, anisotropic geometry (highlighted by the green box labelled “Uniform rod-like”) is the hallmark of crystalline cellulose nanostructures produced under controlled industrial hydrolysis conditions and larger, dense aggregate clusters clearly visible in the upper portion of the micrograph (indicated by red-circle annotations labelled “Aggregate cluster” and “Aggregate”). The coexistence of individualized nanocrystals and micron-scale aggregates in the commercial reference material is well documented in the literature and is attributable to the hygroscopic character of NCC surfaces, which are decorated with sulfate half-ester groups and residual hydroxyl functionalities that engage in extensive inter-particle hydrogen bonding upon drying, driving spontaneous self-assembly into ordered aggregates (Solhi *et al.*, 2023).

NCC derived from pineapple crown leaves (Figure 5b) most closely replicates the morphological features of the commercial reference among the three agricultural residue-derived materials. The green box labelled “Rod-like particles” delineates a region populated by elongated, anisotropic nanocrystals whose aspect ratio and overall geometry are comparable to those of the commercial benchmark, confirming that the high cellulose content of PCL (60.49%) and its relatively low lignin fraction (15.24%) facilitated efficient removal of amorphous domains during acid hydrolysis, thereby liberating intact crystalline segments. However, the yellow box labelled “Rough surface” reveals that the individual particles carry a noticeably textured surface topography absent in the commercial NCC, which may reflect residual surface-bound lignin oligomers or incompletely dissolved hemicellulosic fragments that were not fully eliminated during the alkalization and bleaching pretreatments. In addition, the orange annotation labelled “Size non-uniformity” highlights a heterogeneous distribution of particle dimensions within the field of view, indicating that the hydrolysis conditions, while sufficient to produce rod-like nanocrystals, did not achieve the narrow size dispersity characteristic of optimized industrial processes. A region of macroscale agglomeration is further identified by the red circle labelled “Agglomeration” in the upper right quadrant of the micrograph, arising from the high density of surface sulfate groups and hydroxyl functionalities that drive inter-particle hydrogen bonding upon drying, a phenomenon consistently documented for sulfuric acid-hydrolyzed NCC from diverse lignocellulosic feedstocks (Solhi *et al.*, 2023).



Copyright © 2026, Universitas Sebelas Maret, ISSN 1412-4092, e ISSN 2443-4183

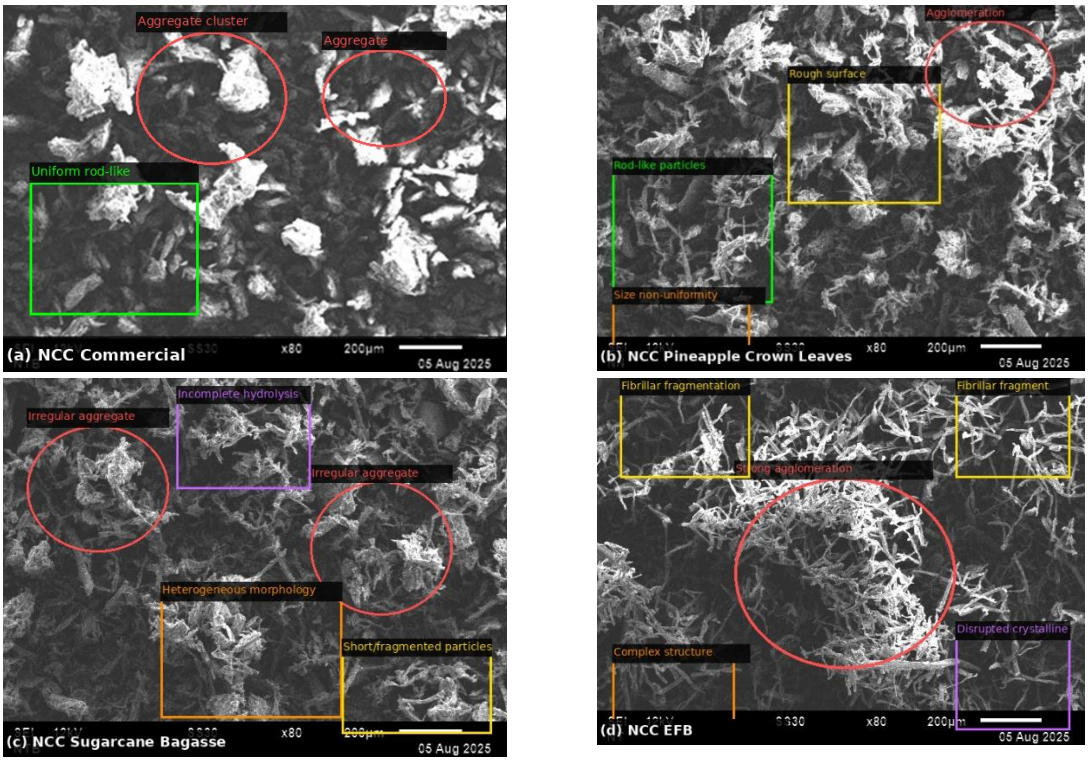



**Figure 5**. SEM (a) NCC commercial, (b) NCC pineapple crown leaves, (c) sugarcane bagasse, and (d) Oil palm empty fruit bunch (EFB) fibers.

NCC from sugarcane bagasse (Figure 5c) exhibits a markedly more disordered morphology relative to both the commercial reference and PCL-NCC. The orange annotation "Heterogeneous morphology" encompasses a broadly distributed field of particles with irregular shapes and dimensions, while two red circles labelled "Irregular aggregate" identify compact, multi-particle clusters that depart substantially from the uniform rod-like habit. The purple box labelled "Incomplete hydrolysis" delineates a region containing coarse, partially unhydrolyzed fibrillar structures whose persistence indicates that the combined alkalization and bleaching sequence was insufficient to fully penetrate and dissolve the hemicellulose-lignin matrix surrounding the cellulose microfibrils in this lignin-rich feedstock (SB lignin content: 39.52%). The yellow box labelled "Short/fragmented particles" further identifies a population of truncated, geometrically irregular fragments, consistent with non-selective over-hydrolysis of partially accessible crystalline domains at fibrillar defect sites. Collectively, these features confirm that the elevated lignin and hemicellulose burden in sugarcane bagasse impedes uniform reagent diffusion during both pretreatment and acid hydrolysis, yielding NCC with inferior morphological regularity and correspondingly reduced crystallinity (CrI = 70.25%) relative to PCL-NCC.

NCC from oil palm EFB (Figure 5d) displays the most structurally complex and morphologically disrupted surface among the four samples, reflecting the dense, highly cross-linked vascular fiber architecture characteristic of monocotyledonous palm tissue (Aprilia *et al.*, 2025). The two yellow boxes labelled "Fibrillar fragmentation" and "Fibrillar fragment" identify extensive fiber-level disintegration across multiple field regions, manifesting as elongated but irregularly fractured fibrillar remnants that lack the geometric regularity of rod-like nanocrystals. A large red-circle annotation labelled "Strong agglomeration" in the central field of the micrograph reveals that these fragmented fibrillar units have coalesced into a massive, densely packed aggregate cluster far exceeding in scale those observed for the commercial or PCL-derived materials. The orange annotation "Complex structure" at the lower left highlights the inherently multiphase, heterogeneous texture of EFB-derived NCC, a direct consequence of the high hemicellulose (28.08%) and lignin (32.14%) contents, which resist complete removal during chemical pretreatment, creating persistent structural heterogeneities within the extracted nanocrystal population. The purple box labelled "Disrupted crystalline" at the lower right delineates localized regions of deformed or fractured crystal domains, consistent with the partial mechanical disruption of cellulose Iβ crystallite packing at points of high shear stress during acid hydrolysis, which accounts for the lowest crystallinity index (CrI = 68.31%) and thermal onset temperature ($T_{onset}$ = 280 °C) recorded among all samples in this study.



Copyright © 2026, Universitas Sebelas Maret, ISSN 1412-4092, e ISSN 2443-4183

Taken together, the SEM analysis provides compelling visual corroboration of the structure–composition–property relationships established by the preceding characterization techniques. Pineapple crown leaves, by virtue of their high cellulose content and low lignin loading, yield NCC with a morphology of rod-like particles, moderate surface roughness, and limited agglomeration that most closely approaches the commercial benchmark. Sugarcane bagasse and EFB, penalized by their elevated lignin and hemicellulose fractions, produce nanocrystals with progressively greater morphological heterogeneity, fibrillar fragmentation, and macroscale aggregation. These observations, in conjunction with the XRD crystallinity data and TGA thermal stability rankings, firmly establish the compositional hierarchy PCL > SB > EFB as the determinant of NCC quality from tropical agricultural residues processed under identical acid hydrolysis conditions.

## CONCLUSION

This study demonstrated that feedstock lignocellulosic composition is the primary determinant of NCC quality when processing oil palm empty fruit bunch (EFB), sugarcane bagasse (SB), and pineapple crown leaves (PCL) under identical alkaline pretreatment, bleaching, and sulfuric acid hydrolysis conditions. PCL, possessing the highest cellulose content (60.49%) and lowest lignin fraction (15.24%), yielded the highest NCC recovery (70.37 ± 1.10%), crystallinity index (73.57%), and thermal decomposition onset temperature (291 °C), with rod-like particle morphology closely resembling commercial NCC. Conversely, SB and EFB produced lower NCC yields (33.23 ± 1.86% and 36.17 ± 0.91%), reduced crystallinity indices (70.25% and 68.31%), lower thermal onset temperatures (285 °C and 280 °C), and morphologically heterogeneous particles characterized by fibrillar fragmentation and pronounced agglomeration, attributable to their elevated lignin and hemicellulose burdens. FTIR analysis confirmed effective removal of non-cellulosic components across all feedstocks, while TGA revealed that thermal stability closely parallels the crystallinity hierarchy (PCL > SB > EFB). These findings establish pineapple crown leaves as the most efficient tropical agricultural residue for sustainable NCC production under mild hydrolysis conditions. Future studies should investigate optimized multi-stage delignification strategies for high-lignin feedstocks and evaluate PCL-derived NCC as a reinforcing agent in polymer nanocomposite applications.

## CONFLICT OF INTEREST

The authors declare that they have no competing financial or personal interests that could have influenced the work reported in this article.

## AUTHOR CONTRIBUTIONS

MM: Funding acquisition, Conceptualization, Supervision, Validation, and Editing and Reviewing the original manuscript; EMM: Project Administration, Investigation, and Manuscript Review; KR: Methodology, Data curation, Resources, Manuscript Drafting, and Editing; EM: Formal Analysis and Manuscript Review; FF: Formal Analysis and Manuscript Review.

## ACKNOWLEDGEMENT

The authors gratefully acknowledge financial support from the Ministry of Higher Education, Science, and Technology, Indonesia, for its financial support for the work described through the Penelitian Dosen Pemula Scheme (grant number: 134/C3/DT.05.00/PL/2025, 40/LL13/AL.04/AKA.PL/2025, 030/LPPM-USM/VI/2025).

## DECLARATION OF GENERATIVE AI

During the preparation of this manuscript, the authors used ChatGPT to assist with English-language editing and grammar improvement. The authors reviewed and edited the AI-assisted language suggestions, verified the scientific content, and take full responsibility for the content of the published article.

## REFERENCES

Akhlaq, M., Maqsood, H., Uroos, M., and Iqbal, A., 2022. A Comparative Study of Different Methods for Cellulose Extraction from Lignocellulosic Wastes and Conversion into Carboxymethyl Cellulose. *ChemistrySelect* 7, e202201533. https://doi.org/10.1002/slct.202201533.

Akinjokun, A.I., Petrik, L.F., Ogunfowokan, A.O., Ajao, J., and Ojumu, T.V., 2021. Isolation and Characterization of Nanocrystalline Cellulose from Cocoa Pod Husk (CPH) Biomass Wastes. *Heliyon* 7, e06680. https://doi.org/10.1016/j.heliyon.2021.e06680.



Copyright © 2026, Universitas Sebelas Maret, ISSN 1412-4092, e ISSN 2443-4183

Almashhadani, A.Q., Leh, C.P., Chan, S.-Y., Lee, C.Y., and Goh, C.F., 2022. Nanocrystalline Cellulose Isolation Via Acid Hydrolysis from Non-Woody Biomass: Importance of Hydrolysis Parameters. *Carbohydrate Polymers* 286, 119285. https://doi.org/10.1016/j.carbpol.2022.119285.

Alsuwait, R.B., Bakare, A.O., Souiyah, M., Ganiyu, S.A., and Momohjimoh, I., 2024. Effect of Treatment Conditions on the Morphology of Date Empty Fruit Bunch Lignocellulosic Fiber for Biocomposite Applications. *Carbohydrate Polymer Technologies and Applications* 7, 100519. https://doi.org/10.1016/j.carpta.2024.100519.

Alvarado, M.C., Ignacio, M.C.C.D., Acabal, M.C.G., Lapuz, A.R.P., and Yaptenco, K.F., 2024. Review on Nanocellulose Production from Agricultural Residue through Response Surface Methodology and Its Applications. *Nano Trends* 8, 100054. https://doi.org/10.1016/j.nwnano.2024.100054.

Ansari, M.M., Heo, Y., Do, K., Ghosh, M., and Son, Y.-O., 2024. Nanocellulose Derived from Agricultural Biowaste by-Products–Sustainable Synthesis, Biocompatibility, Biomedical Applications, and Future Perspectives: A Review. *Carbohydrate Polymer Technologies and Applications* 8, 100529. https://doi.org/10.1016/j.carpta.2024.100529.

Aprilia, S., Fathanah, U., Meilina, H., Djuned, F., Hisbullah, H., Rahmah, K., Zuwanna, I., Rinaldi, W., and Amin, A., 2025. Modification of Polyether Sulfone Ultrafiltration Membranes by Adding Nanocellulose and Silica as Additives Based on Agricultural Solid Waste. *Journal of Membrane Science and Research*, https://doi.org/10.22079/jmsr.2025.2054708.1709.

D'acierno, F., Michal, C.A., and Maclachlan, M.J., 2023. Thermal Stability of Cellulose Nanomaterials. *Chemical Reviews* 123, 7295–7325. https://doi.org/10.1021/acs.chemrev.2c00816.

Dimawarnita, F., Faramitha, Y., Prakoso, H.T., Puspitasari, I., Kalbuadi, D.N., and Prasetyo, D., 2023. Characterization of Cellulose from Oil Palm Empty Fruit Bunches by Fast Delignification Process with Different Solvents. *E-Journal Menara Perkebunan* 91, https://doi.org/10.22302/mp.v91i2.542.

Dungani, R., Melani, L., Fatriasari, W., Munawar, S.S., Syamani, F.A., Mahardika, M., Karliati, T., Dewi, M., Alpian, and Supriyati, W., 2023. Kenaf Bast Nanocrystalline Cellulose: Analysis of Morphological, Chemical, Crystalline, and Thermal. *BioResources* 18, 6913–6928. https://doi.org/10.15376/biores.18.4.6913-6928.

Faria, L.U.S., Pacheco, B.J.S., Oliveira, G.C., and Silva, J.L., 2020. Production of Cellulose Nanocrystals from Pineapple Crown Fibers through Alkaline Pretreatment and Acid Hydrolysis under Different Conditions. *Journal of Materials Research and Technology* 9, 12346–12353. https://doi.org/10.1016/j.jmrt.2020.08.093.

Fitriani, F., Aprilia, N.A.S., and Arahman, N., 2020. Properties of Nanocrystalline Cellulose from Pineapple Crown Leaf Waste. *IOP Conference Series: Materials Science and Engineering* 796, 012007. https://doi.org/10.1088/1757-899X/796/1/012007.

Fitriani, F., Aprilia, S., Arahman, N., and Bilad, M.R., 2022. Effect of Acid Concentration on the Properties of Microcrystalline Cellulose from Pineapple Crown Leaf. *Jurnal Rekayasa Kimia & Lingkungan* 17, 1–7. https://doi.org/10.23955/rkl.v17i1.21010.

Fitriani, F., Aprilia, S., Arahman, N., Bilad, M.R., Amin, A., Huda, N., and Roslan, J., 2021. Isolation and Characterization of Nanocrystalline Cellulose Isolated from Pineapple Crown Leaf Fiber Agricultural Wastes Using Acid Hydrolysis. *Polymers* 13, 4188. https://doi.org/10.3390/polym13234188.

Harahap, M., Daulay, N., Zebua, D., and Gea, S., 2023. Nanofiber Cellulose/Lignin from Oil Palm Empty Fruit Bunches and the Potential for Carbon Fiber Precursor Prepared by Wet-Spinning. *International Journal of Technology* 14, 152. https://doi.org/10.14716/ijtech.v14i1.5082.

Hemida, M.H., Moustafa, H., Mehanny, S., Morsy, M., Dufresne, A., Abd El Rahman, E.N., and Ibrahim, M.M., 2023. Cellulose Nanocrystals from Agricultural Residues (*Eichhornia crassipes*): Extraction and Characterization. *Heliyon* 9, e16436. https://doi.org/10.1016/j.heliyon.2023.e16436.

Hidayatulloh, I., Abdulloh, S.H., and Lidya, E., 2025. A One-Pot Method for the Synthesis of Nanocellulose from Palm Oil Empty Bunches Using Fe-Cr Combination Catalyst. *ASEAN Journal of Chemical Engineering* 25, 11–22. https://doi.org/10.22146/ajche.12037.

Hidayatulloh, I., Widyanti, E.M., Kusumawati, E., and Elizabeth, L., 2021. Nanocellulose Production from Empty Palm Oil Fruit Bunches (Epofb) Using Hydrolysis Followed by Freeze Drying. *ASEAN Journal of Chemical Engineering* 21, 52. https://doi.org/10.22146/ajche.61093.

Khan, A., Jawaid, M., Kian, L.K., Khan, A.A.P., and Asiri, A.M., 2021. Isolation and Production of Nanocrystalline Cellulose from Conocarpus Fiber. *Polymers* 13, 1835. https://doi.org/10.3390/polym13111835.



Copyright © 2026, Universitas Sebelas Maret, ISSN 1412-4092, e ISSN 2443-4183

Liu, W., Liu, K., Du, H., Zheng, T., Zhang, N., Xu, T., Pang, B., Zhang, X., Si, C., and Zhang, K., 2022. Cellulose Nanopaper: Fabrication, Functionalization, and Applications. *Nano-Micro Letters* 14, 104. https://doi.org/10.1007/s40820-022-00849-x.

Madhushree, M., Vairavel, P., Mahesha, G., and Bhat, K.S., 2024. A Comprehensive Review of Cellulose and Cellulose-Based Materials: Extraction, Modification, and Sustainable Applications. *Journal of Natural Fibers* 21, 2418357. https://doi.org/10.1080/15440478.2024.2418357.

Magalhães, S., Fernandes, C., Pedrosa, J.F.S., Alves, L., Medronho, B., Ferreira, P.J.T., and Rasteiro, M.D.G., 2023. Eco-Friendly Methods for Extraction and Modification of Cellulose: An Overview. *Polymers* 15, 3138. https://doi.org/10.3390/polym15143138.

Mahmud, M.A., and Anannya, F.R., 2021. Sugarcane Bagasse - a Source of Cellulosic Fiber for Diverse Applications. *Heliyon* 7, e07771. https://doi.org/10.1016/j.heliyon.2021.e07771.

Mishra, S., Prabhakar, B., Kharkar, P.S., and Pethe, A.M., 2023. Banana Peel Waste: An Emerging Cellulosic Material to Extract Nanocrystalline Cellulose. *ACS Omega* 8, 1140–1145. https://doi.org/10.1021/acsomega.2c06571.

Mtibe, A., John, M.J., Andrew, J.E., and Mokhena, T.C., 2022. Sequential Extraction of Carbohydrates and Lignin from Agricultural Waste and Their Structural Characterization. *Biomaterials and Polymers Horizon* 1, https://doi.org/10.37819/bph.001.02.0216.

Nahurira, J., Gorfad, R.S., and Mayani, S.V, 2024. A Recent Overview on Agro Waste Based Nano Cellulose Composite and Its Environmental Application: A Short Review. *RASAYAN Journal of Chemistry* 17, 118–127. https://doi.org/10.31788/RJC.2024.1718655.

Pérez, R.H., Delgado, R.S., Paredes, A.O., Delgado, A.S., Hernández, E.G., Valis, A.M., and Candia, F.M., 2022. Comparing Acid and Enzymatic Hydrolysis Methods for Cellulose Nanocrystals (CNCs) Obtention from Agroindustrial Rice Husk Waste. *Journal of Nanotechnology* 2022, 1–11. https://doi.org/10.1155/2022/5882113.

Qureshi, S.S., Nizamuddin, S., Xu, J., Vancov, T., and Chen, C., 2024. Cellulose Nanocrystals from Agriculture and Forestry Biomass: Synthesis Methods, Characterization and Industrial Applications. *Environmental Science and Pollution Research* 31, 58745–58778. https://doi.org/10.1007/s11356-024-35127-3.

Rodzi, S.M., Azizan, A., Rahman, N.A., Gen, M., and Bakar, N.F.A., 2024. Microcrystalline Cellulose Production from Pineapple Leaves and Crowns Using Trifluoroacetic Acid. *Malaysian Journal of Chemistry* 26, https://doi.org/10.55373/mjchem.v26i5.338.

Sartika, D., Firmansyah, A.P., Junais, I., Arnata, I.W., Fahma, F., and Firmanda, A., 2023. High Yield Production of Nanocrystalline Cellulose from Corn Cob through a Chemical-Mechanical Treatment under Mild Conditions. *International Journal of Biological Macromolecules* 240, 124327. https://doi.org/10.1016/j.ijbiomac.2023.124327.

Sayakulu, N.F., and Soloi, S., 2022. The Effect of Sodium Hydroxide (Naoh) Concentration on Oil Palm Empty Fruit Bunch (Opefb) Cellulose Yield. *Journal of Physics: Conference Series* 2314, 012017. https://doi.org/10.1088/1742-6596/2314/1/012017.

Shen, P., Tang, Q., Chen, X., and Li, Z., 2022. Nanocrystalline Cellulose Extracted from Bast Fibers: Preparation, Characterization, and Application. *Carbohydrate Polymers* 290, 119462. https://doi.org/10.1016/j.carbpol.2022.119462.

Solhi, L., Guccini, V., Heise, K., Solala, I., Niinivaara, E., Xu, W., Mihhels, K., Kröger, M., Meng, Z., Wohlert, J., Tao, H., Cranston, E.D., and Kontturi, E., 2023. Understanding Nanocellulose–Water Interactions: Turning a Detriment into an Asset. *Chemical Reviews* 123, 1925–2015. https://doi.org/10.1021/acs.chemrev.2c00611.



Copyright © 2026, Universitas Sebelas Maret, ISSN 1412-4092, e ISSN 2443-4183